Volume 40 http://acousticalsociety.org/

International Conference on Underwater Acoustics

9 September 2020

Parallel Session 4A - Radiated Noise 14:45

The effect of water surface roughness on the measurement of radiated ship noise

He Tengjiao
College of Underwater Acoustic Engineering, Harbin Engineering University, Harbin, Heilongjiang 150001, CHINA; hetengjiao22547@126.com

Victor F. Humphrey
Institute of Sound and Vibration Research, University of Southampton Faculty of Physical Sciences and Engineering, Southampton, Hampshire, SO17 1BJ, UNITED KINGDOM, vh@isvr.soton.ac.uk

Shiqi Mo and Erzheng Fang
College of Underwater Acoustic Engineering, Harbin Engineering University, Harbin, Heilongjiang 150001, CHINA; moshiqi@hrbeu.edu.cn; fangerzheng@hrbeu.edu.cn

As a result of the increased interest in the potential environmental impact of noise from shipping several international standards have been developed for determining the radiated noise level and equivalent monopole source level of vessels. It is important to understand the systematic errors and uncertainties associated with such techniques. One potential issue is the effect of water surface roughness on the measured radiated noise. The roughness reduces the amplitude of the coherent reflection from the sea surface and therefore reduces the impact of Lloyd's Mirror effect at higher frequencies. In order to investigate this further two cases are considered: a deep water case with translationally symmetric surface waves and a shallow water case with a two-dimensional rough sea surface. The deep and shallow water cases are simulated using an equivalent source method based model and a three-dimensional Helmholtz-Kirchhoff approximation, respectively. The results indicate that the incoherent scattering component almost completely compensates for the coherent component loss. The variation in the results for different sea surface implementations indicates how the sensitivity of the measurement varies with frequency.

Published by the Acoustical Society of America

 https://doi.org/10.1121/2.0001346

1. INTRODUCTION

Recently there has been growing interest in underwater anthropogenic noise for environmental reasons. As a significant contribution to underwater anthropogenic noise, shipping noise potentially poses a threat to marine fauna by interfering with their behavior by affecting communication, feeding and predation. Driven by the motivation to protect marine fauna from the adverse impact of shipping noise, the production of underwater noise maps has become a major means of guiding noise mitigation. This requires precise assessments of the underwater radiated noise (URN) from vessels. The issue of URN measurements has been identified as one requiring further research, as indicated by several recent collaborative projects, such as AQUO (Achieve Quieter Oceans)[1,2] and SONIC (Suppression Of underwater Noise Induced by Cavitation)[3] launched by the EU (European Union).

For standardizing the procedures of URN measurements, the International Organization for Standardization (ISO) has issued the ISO 17208-1 standard,[4] in which three hydrophones, placed at a distance of d_{CPA} from the vessel track at the closest point of approach (CPA), are used to mitigate some aspects of the water surface reflection, as shown in Fig. 1. The received levels (RLs) at the hydrophones are converted to the radiated noise level (RNL) by simply correcting for geometrical spreading assuming spherical spreading. A second standard (ISO-17208-2)[5] introduces a correction factor to obtain the source level (SL) from the radiated noise level. One strong assumption made in the ISO 17208-2 standard is that the water surface is flat, which can be violated easily in practice. The water surface can be randomly rough, or even periodic, in the real ocean driven by wind forcing. Sound scattering from the rough water surface, therefore, affects the RNL at high frequencies (above 1 kHz), potentially preventing the Lloyd's Mirror correction from being used directly.

The effects of sound scattering from rough water surfaces on URN measurements have been numerically investigated by Audoly and Meyer using an image model.[6] The roughness of the water surface was considered in the model by introducing a coherent reflection coefficient which reduces the magnitude of the water surface reflection. The specular reflection is, therefore, taken into account, while the component due to scattering (the incoherent field) representing the non-specular reflection is excluded. The absent incoherent field is vital for sound propagation in the near-field region where the URN measurements are focused. Further investigation needs to be undertaken to study the effects of surface scattering on URN measurements with a model offering a full-wave solution for the wavefield.

This paper presents a numerical study of the effects of sound scattering from rough water surfaces on URN measurements. Two scenarios are considered: a deep water case with translationally symmetric surface waves and a shallow water case with a two-dimensional rough sea surface. The deep and shallow water cases are simulated using an equivalent source method based model[9] and a three-dimensional Helmholtz-Kirchhoff approximation, respectively. In the deep water case, the source-receiver configuration follows the recommendation in the ISO 17208-1 standard as shown in Fig. 1. The remainder of this paper is organized as follows. Section 2 describes the modelling method before Section 3 presents numerical results and discussion. Finally, the conclusions of this study are summarized in Section 4.

2. METHOD

A. UNDERWATER RADIATED NOISE MEASUREMENT MODEL

To simulate the URN measurements, the source-receiver configuration follows the recommendation of the ISO 17208-1 standard,[4] with the vessel modelled as a monopole point source placed at a depth of d_s, as shown in Fig. 1. Three hydrophones vertically immersed at depths of d_{Hi} (i=1, 2 or 3) are placed at a CPA distance of d_{cpa} from the vessel track. The data window (DW) shown in Fig. 2 (a) is the portion of the track, truncated by two points at an angle of $\pm 30^\circ$ to the line linking the CPA point and hydrophone array,[4] used

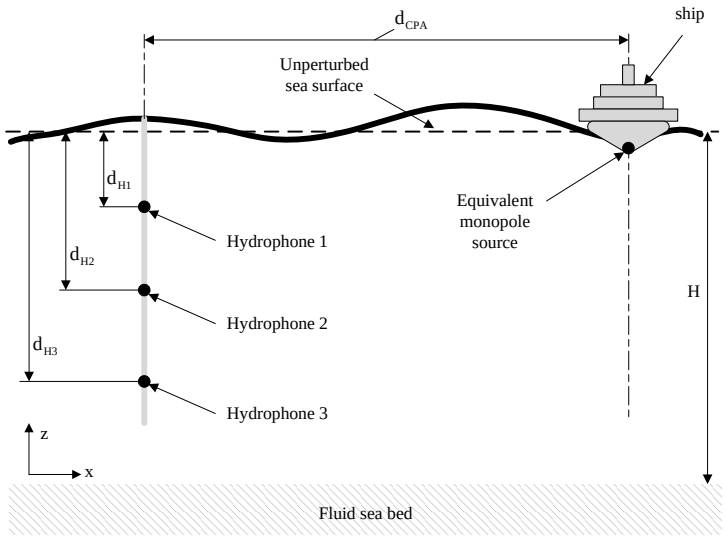

Figure 1: The hydrophone setup geometry for URN measurements in the $x-z$ plane.

in the data analysis. The evaluation of the RNL of the vessel starts with the power average of the narrowband pressure across a series of sub-sections into which the DW is divided. Then, one-third octave (OTO) band levels are obtained by integrating the narrowband results across each OTO band. Finally, the average across the three hydrophones gives the RNL of the vessel, after correcting for spherical spreading.

In this paper, the signal recorded by the hydrophone array for a moving source is replaced with a spatial scan by the hydrophone array while the source is static as shown in Fig. 2 (b). Such a conversion is reasonable due to the negligible Doppler effects after performing the frequency average across OTO bands. The DW in the quasi-static model is defined as the scanning path extending $\pm 30^{\circ}$ either side of the CPA point. For each run, the pressure field at the hydrophone array in the quasi-static model is calculated using either the ESM-based model or the 3D HKA model introduced in Section 2C. Here, multiple implementations of the wind-generated sea surfaces are required to study the scattering effects, and thus the ensemble average of the fields over the different implementations should be performed ahead of the average across the DW for individual runs. The evaluation of the RNL of the vessel for each hydrophone can be found from:

$$RNL = RL + 20\log_{10}(\frac{d_{total}}{r_{ref}}), \tag{1}$$

where d_{total} is the slant range from the source to the hydrophone, r_{ref}= 1m and RL is the received level:

$$RL = 10\log_{10}(\frac{1}{N_f}\sum_{f}\frac{1}{N_\alpha}\sum_{\alpha}<|p_i(f,\alpha)|^2>), \tag{2}$$

with $<\bullet>$, $\sum_f \bullet$ and $\sum_\alpha \bullet$ representing the ensemble average over different rough surface implementations, and the summation across OTO bands and DW sections, respectively. Here, N_f and N_α are the numbers of frequency samples in each OTO band and sub-sections in the DW, and $p_i(f,\alpha)$ is the sound pressure received by i^{th} hydrophone at an angle of α to the line linking the CPA point and source at frequency f. Note that, the theoretical RNL of a point source is 0 dB, and thus the RNL calculated by Eq. (1) also represents the correction factor (CF) that needs to be subtracted from a RNL measurement to compensate for the real transmission loss when deducing the equivalent source level of the vessel.

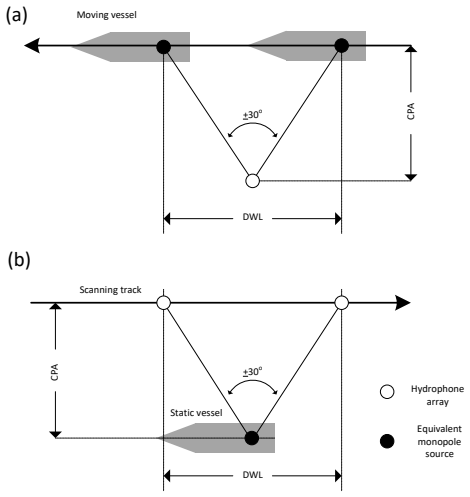

Figure 2: (a) The vessel manoeuver during trials and (b) The quasi-static model of the simulated trial.

B. ROUGH SEA SURFACE MODEL

A wind speed- and fetch length-dependent model, the Joint North Sea Wave Project (JONSWAP)[7] spectra, is utilized to model the wind-generated surfaces. The 2-D surface is calculated by assuming azimuthal symmetry of the 1-D JONSWAP spectra about (k_x, k_y). Here, k_x and k_y are the 2-D wavenumbers. Note that, the JONSWAP spectra in the wavenumber domain is converted from that in the frequency domain using the dispersion relation for shallow water[8] . After multiplying $S(k_x, k_y)$ by the cos-squared spreading factor $\cos^2(\theta)$ where θ is the phase angle of $k_x + ik_y$, the 2-D surface height distribution is realized using the 2-D Fourier transform. The default fetch length was set to be 10 km in this paper.

C. ACOUSTIC PROPAGATION MODEL

The 3-D pressure field $p_i(f, \alpha)$ is calculated using an ESM-based model for the deep water case with translationally symmetric surfaces and using the 3-D Helmholtz-Kirchhoff approximation (HKA) for the shallow water case with 2-D rough surfaces. Details of the ESM-based model will not be presented, but can be seen in Ref.[9]

The derivation of the 3-D HKA is summarized here. The starting point is to consider the Helmholtz integral equation applied to the sound field below a pressure-release boundary,[10] with the scattered field given by:

$$p_s(\boldsymbol{r}_d, \boldsymbol{r}) = \int_\Gamma G(\boldsymbol{r}_\Gamma, \boldsymbol{r}) \frac{\partial p(\boldsymbol{r}_d, \boldsymbol{r}_\Gamma)}{\partial n} d\Gamma, \tag{3}$$

where $G(\boldsymbol{r}_\Gamma, \boldsymbol{r})$ is the water/seabed half-space Green's function for the shallow water case. A complex image method[11] is used to calculated the Green's function. The complex image method is capable of handling the cases of the fluid seabed with two homogenous layers, and only a few orders of complex images are required to provide a good accuracy.[11] In this paper, 5 orders of complex images were used for the case of shallow water. $\frac{\partial p(\boldsymbol{r}_\Gamma, \boldsymbol{r})}{\partial n}$ is the normal derivative of the total pressure on the rough surface. In the Kirchhoff approximation, it follows:

$$\frac{\partial p(\boldsymbol{r}_d, \boldsymbol{r}_\Gamma)}{\partial n} \simeq 2 \frac{\partial p_{inc}(\boldsymbol{r}_d, \boldsymbol{r}_\Gamma)}{\partial n}. \tag{4}$$

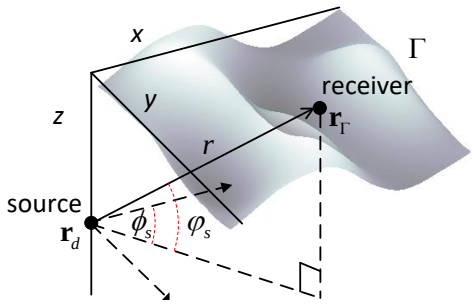

Figure 3: The scheme of the 3-D Helmholtz-Kirchhoff approximation for a 2-D surface.

Here, the normal derivative of the incident field to the rough surface is given by:

$$\frac{\partial p_{inc}(\boldsymbol{r}_d, \boldsymbol{r}_\Gamma)}{\partial n} = \bigtriangledown p_{inc} \bullet \overrightarrow{\boldsymbol{n}} \tag{5}$$

where $\overrightarrow{\boldsymbol{n}}$ is the normal of the rough surface:

$$\overrightarrow{\boldsymbol{n}} = \frac{(- \bigtriangledown \eta, 1)}{\sqrt{1 + (\bigtriangledown \eta)^2}}, \tag{6}$$

and η is the wave height function of x and y. The integral in Eq. (3) then becomes:

$$\begin{aligned} p_s(\boldsymbol{r}_d, \boldsymbol{r}) =& 2 \iint w G_{3D}(\boldsymbol{r}_\Gamma, \boldsymbol{r}) (- \frac{\partial p_{inc}(\boldsymbol{r}_d, \boldsymbol{r}_\Gamma)}{\partial r} \frac{\partial \eta}{\partial x} \cos\psi_s \cos\phi_s \\ & - \frac{\partial p_{inc}(\boldsymbol{r}_d, \boldsymbol{r}_\Gamma)}{\partial r} \frac{\partial \eta}{\partial y} \cos\psi_s \sin\phi_s + \frac{\partial p_{inc}(\boldsymbol{r}_d, \boldsymbol{r}_\Gamma)}{\partial z}) dx dy, \end{aligned} \tag{7}$$

where $w = 1 \,/\, \sqrt{1 + (\bigtriangledown \eta)^2}$; ϕ_s and ψ_s, shown in Fig. 3, are the azimuth and elevation angle of the incident sound wave. To evaluate the integral in Eq. (7) numerically, the 2D rough sea surfaces are truncated at $x = \pm 125$ m and $y = \pm 125$ m with the point source as the origin. Even discretization of the surface is applied in both the x-axis and y-axis directions with 5 points per wavelength, guaranteeing the accuracy of the HKA.

3. NUMERICAL SIMULATION

A. SIMULATION PARAMETERS

For evaluating the correction factor (CF), OTO bands covering the range from 31.5 Hz to 10 kHz were considered with $N_f = 21$ per band, and the DW was divided into 13 sections with an α increment of 5° initially ($N_\alpha = 13$). The ensemble average CF in the presence of wind-generated rough surfaces, and its associated uncertainties, were evaluated over 30 implementations of random rough sea surfaces. Simulations were carried out using the default environmental parameters and configuration shown in Table. 1. The seafloor was assumed to be level and flat.

B. RESULTS AND DISCUSSION

i. Deep water case

Figure. 4 displays the correction factors (CFs) for the total, coherent and incoherent fields for various wind speeds. The CFs for the total field vary rapidly with frequency below 100 Hz as a result of the dipole

Table 1: Environment Parameters and source-receiver configuration.

Parameter	Deep water	Shallow water
Source depth (m/s) d_s	4	4
CPA Distance (m) d_{cpa}	100	100
Top hydrophone depth (m) d_{H1}	26.8	15
Middle hydrophone depth (m) d_{H2}	57.7	35
Bottom hydrophone depth (m) d_{H3}	100	55
Water sound speed (m/s) c_1	1490	1490
Water density (kg/m^3) ρ_1	1000	1000
Seabed sound speed (m/s) c_2	/	1749
Seabed attenuation (dB/ λ) α_2	/	0.9
Seabed density (kg/m^3) ρ_2	/	1941

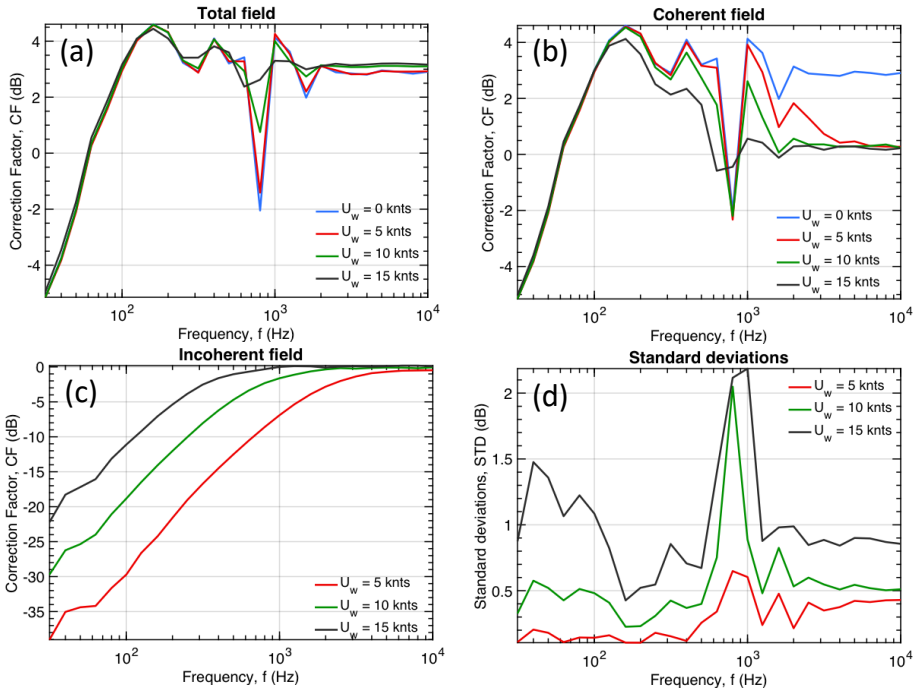

Figure 4: Correction factors of the (a) total, (b) coherent and (c) incoherent fields, and (d) the associated standard deviations, for wind speeds of 0 knots, 5 knots, 10 knots and 15 knots in deep water.

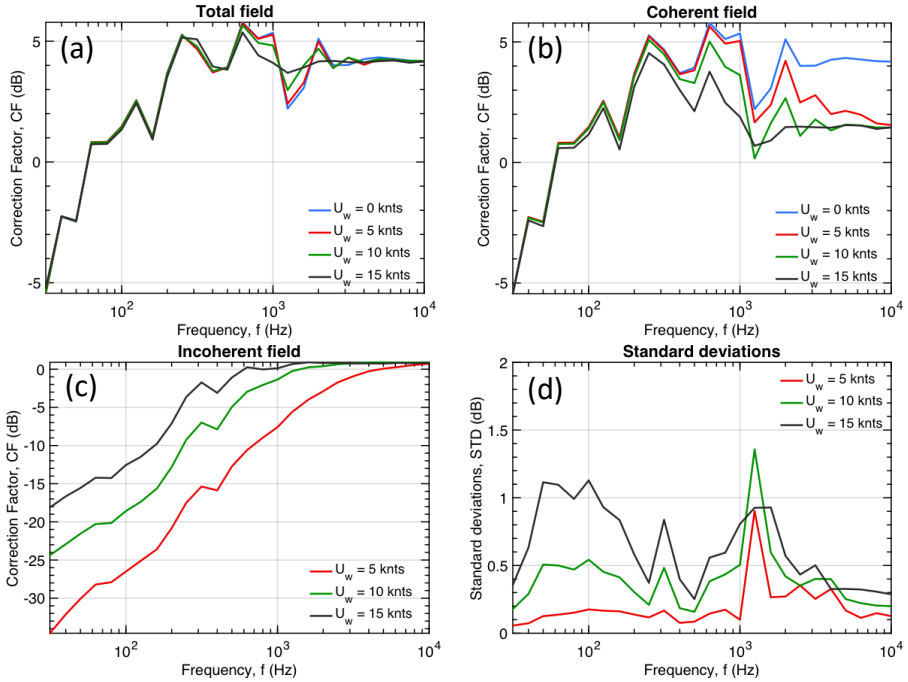

Figure 5: Correction factors of the (a) total, (b) coherent and (c) incoherent fields, and (d) the associated standard deviations, for wind speeds of 0 knots, 5 knots, 10 knots and 15 knots in shallow water.

effect produced by the source and its image due to the water surface. At higher frequencies fluctuations are observed, decreasing as the wind speed increases for the frequencies ranging from 100 Hz to 2000 Hz. Above 2000 Hz, the CFs for the total field approach a relatively constant value of around 3 dB. For non-zero wind speed, the CFs for the coherent field gradually reduce to 0 dB as the frequency increases, decreasing more rapidly for stronger wind intensities. This is caused by the scattering effects which are intensified by the increase in the roughness of the water surfaces due to the increased wind speed. Consequently, the coherent field representing the specular reflection is weakened, which coincides with the reduction of the Lloyds Mirror impact at higher frequencies demonstrated by Audoly.[6] In contrast, the incoherent field representing the scattering component plotted in Fig. 4 (c) shows the opposite behavior to the coherent field, tending to compensate for the coherent loss at higher frequencies. The compensation by the incoherent field explains why the CFs for the total field approach a relatively constant value at higher frequencies.

On the other hand, the standard deviations (STDs) shown in Fig. 4 (d) exhibit an overall increase as the wind speed increases, with pronounced peaks below 100 Hz and at around 1000 Hz; the latter corresponds to the frequency where the hydrophone geometry is not as efficient at cancelling out the Lloyd's Mirror effect, and there is a pronounced dip in the CFs for the total and coherent fields. This indicates that the sensitivity of measurements depends on the source-receiver configuration, so the sensitivity of measurements may be reduced by optimizing the source-receiver configuration to remove such dips.

ii. Shallow water case

For comparison, Fig. 5 gives the relevant results for a shallow water case with the parameters shown in Table 1. In this case, the behaviors of the CFs for the total, coherent and incoherent fields are very similar to those in the deep water case. Note that for high frequencies, the constant value, at which the CFs for the total field remain stable, is increased by 1 dB compared with the deep water case, depending on not only

the source-receiver configuration and CPA distance but also the parameters of the seabed.[12] Also, the peak values of the STDs are reduced to no more than 1.5 dB in the shallow water case, which indicates that the interference between the surface- and seabed-reflections may decrease the sensitivity of measurements. This reflects the less pronounced dips in the CF for the coherent field.

4. CONCLUSION

This paper presents a numerical study of the effects of water surface roughness on the URN measurements. Both a deep water case with translationally symmetric waves and a shallow water case with 2-D rough surfaces have been investigated using an ESM-based model and the 3-D HKA, respectively. The results show that, at higher frequencies, the surface reflection coefficient reduces the coherent field and, hence, the correction factor. Nevertheless, scattering becomes significant at higher frequencies. Including the scattered field component results in the correction factor being relatively constant at higher frequencies. The presented results ignore bubble scattering, which will potentially introduce attenuation as well as scattering and consequently affects the correction factor at higher frequencies.

REFERENCES

[1] Audoly, C *et al.*, "Mitigation of underwater radiated noise related to shipping and its impact on marine life: A practical approach developed in the scope of AQUO project", *IEEE Journal of Oceanic Engineering.* **42**(2), 373-387 (2017).

[2] Audoly, C and Rizzuto, E, "AQUO: Achieve quieter oceans by shipping noise footprint reduction FP7-collaborative project No 314227 WP 2:Noise sources, Task T2.1,"Ship underwater radiated noise patterns"", $(http://www.aquo.eu/downloads/AQUO\_R2.9\_Ship\_URN\_Patterns\_V1.0.pdf)$ (2015).

[3] Prins *et al.*, "Suppression of underwater noise induced by cavitation: SONIC", *Transportation Research Procedia.* **14**, 2668-2677 (2016).

[4] ISO, "Underwater acoustics — Quantities and procedures for description and measurement of underwater sound from ships — Part 1: Requirements for precision measurements in deep water used for comparison purposes", *ISO 17208-1, International Standardization Organization, Geneva, 2016*, (2016).

[5] ISO, "Underwater acoustics — Quantities and procedures for description and measurement of underwater sound from ships — Part 2: Determination of source levels from deep water measurements", *ISO 17208-2, International Standardization Organization, Geneva, 2019*, (2019).

[6] Audoly, C and Meyer, V, "Measurement of radiated noise from surface ships-influence of the sea surface reflection coefficient on the Lloyd's mirror effect", *Proceedings of Acoustics Australia 2017, Perth, Australia, November 2017*, (2017).

[7] Hasselmann *et al.*, "Measurements of wind-wave growth and swell decay during the joint north sea wave project (JONSWAP)", *Ergänzungsheft.* 8-12 (1973).

[8] Ballard, M. S, "Three-dimensional acoustic propagation under a rough sea surface", *Proceedings of Meetings on Acoustics ICA2013, Acoustical Society of America.* **19, p.** 070077 (2013).

[9] He *et al.*, "Three-dimensional sound scattering from transversely symmetric surface waves in deep and shallow water using the equivalent source method", *The Journal of the Acoustical Society of America.* **148**(1), 73-84 (2020).

[10] Thorsos, E. I, "The validity of the Kirchhoff approximation for rough surface scattering using a gaussian roughness spectrum", *The Journal of the Acoustical Society of America.* **83**(1), 78-92 (1988).

[11] Fawcett, J. A, "Complex-image approximations to the half-space acousto-elastic Green's function", *The Journal of the Acoustical Society of America.* **108**(6), 2791-2795 (2000).

[12] Meyer, V and Audoly, C, "A parametric study of the environment and the array configuration for underwater noise measurement from ships in shallow water", *Proceedings of the 26th International Congress on Sound and Vibration.* (2019).